DOI: 10.15244/pjoes/210690

ONLINE PUBLICATION DATE: 2025-12-01

Original Research

# Sorption Behaviors and Mechanisms of Cadmium on Polypropylene, Bamboo Biochar, and Rice Husk Ash in Aqueous Solutions

Nantira Vorakarnchanabun<sup>1</sup>, Suchanya Wongrod<sup>1,20\*</sup>, Sasidhorn Buddhawong<sup>1</sup>

<sup>1</sup>Environmental Technology Program, School of Energy, Environment and Materials, King Mongkut's University of Technology Thonburi, Bangkok 10140, Thailand <sup>2</sup>Environmental and Energy Management for Community and Circular Economy (EEC&C) Research Group, King Mongkut's University of Technology Thonburi, Bangkok 10140, Thailand

> Arrived: 2 May 2025 Accepted: 13 September 2025

## **Abstract**

This study investigated the adsorption behavior and mechanisms of cadmium ions (Cd2+) from aqueous solutions on virgin polypropylene (PP<sub>0</sub>), 1-to-3-week aged polypropylene (PP<sub>1</sub>, PP<sub>2</sub>, and PP<sub>3</sub>), bamboo biochar (BBC), and rice husk ash (RHA). Adsorption kinetic and isotherm experiments were conducted to evaluate the performance of each material. Fourier-transform infrared spectroscopy and Brunauer-Emmett-Teller analyses revealed the presence of hydroxyl and carboxyl functional groups and microporous structures, respectively, on the adsorbent surfaces. The pH of the point of zero charge analysis indicated that the surfaces of PPo-PP, carried net negative charges at a pH solution of 7.0±0.1, whereas BBC and RHA exhibited net positive surface charges under the same conditions. The adsorption kinetics of Cd by PP<sub>0</sub>, PP<sub>1</sub>, PP<sub>2</sub>, PP<sub>3</sub> and BBC followed the pseudo-second-order model ( $R^2 = 0.951$ , 0.963, 0.997, 0.996, and 0.999, respectively), suggesting chemical adsorption as the dominant mechanism. In contrast, the adsorption by RHA was best described by the pseudo-first-order model ( $R^2 = 0.990$ ), indicating a physical adsorption process. Isotherm analysis showed that the Freundlich model provided the best fit for PP<sub>0</sub>-PP<sub>2</sub>, indicating multilayer adsorption on the surfaces. For RHA, the Langmuir model was more suitable, with a maximum adsorption capacity of 815.02 µg/g, implying monolayer adsorption on the surface. Overall, BBC and RHA demonstrated significantly higher cadmium adsorption capacities compared to PP<sub>o</sub>-PP<sub>o</sub>, likely due to their much greater surface areas, 42 to 56 times higher than that of the PP. Importantly, this study presents a comparative framework evaluating the sorption behavior of aged polypropylene microplastics in relation to biomass-based adsorbents, focusing on surface transformations during environmental aging and their interactions with heavy metals. These findings confirm the performance of agricultural waste-derived adsorbents and the emerging

Tel.: +66-2470-8655

°ORCID iD: 0000-0001-7192-4989

<sup>\*</sup>e-mail: suchanya.won@kmutt.ac.th

environmental risks posed by co-contamination from aged microplastics and heavy metals in aquatic systems.

Keywords: bamboo biochar, cadmium adsorption, microplastics, polypropylene, rice husk ash

#### Introduction

Cadmium (Cd<sup>2+</sup>) is a highly toxic, non-biodegradable heavy metal, considered among the most hazardous due to its persistence in ecosystems and severe environmental and health risks [1]. Exposure to Cd<sup>2+</sup> can lead to severe health problems such as kidney damage, bone fractures, and cancer [2]. Its contamination in water is a critical concern, as Cd2+ can be entered through various anthropogenic activities, including mining, industrial operations, and improper waste disposal. The contamination of Cd2+ has been reported in the Chao Phraya River Mouth Water, Thailand, with concentrations ranging from 0.029 to 0.193 μg/L [3]. These concentrations of Cd<sup>2+</sup> should not exceed 5  $\mu$ g/L and 50  $\mu$ g/L at water hardness levels of <100 mg/L and >100 mg/L as CaCO<sub>3</sub>, respectively [4]. In addition, Cd2+ has been reported to accumulate in microplastics found in river sediments of the Beijiang River littoral, China, at concentrations of 2.1-17.6 µg/g [5]. These findings highlight the widespread nature of cadmium pollution and provide important evidence that metals can interact with microplastics in the environment.

Microplastics are plastic debris waste with particle sizes smaller than 5 mm and are considered the most abundant in populated coastal and marine ecosystems [6]. They have been found in various environments, ranging from freshwater to seawater. In 2018, their global abundance in oceans was estimated at 268,940 tons, equivalent to about 5.25 trillion particles [7]. The quantity continues to rise alarmingly each year. They can pass through the wastewater treatment process, enter aquatic environments, and thus affect ecosystems [8]. Their relatively lower density than water allows them to float on the surface water or remain suspended in the water column. In addition, microplastics can release toxic additives or concentrate additional toxic chemicals in the environment, such as bacteria or microbial communities, persistent organic pollutants, carcinogens, endocrine-disrupting chemicals, and heavy metals [9-12]. This is due to the large specific surface area and strong hydrophobicity, which can ultimately affect the organisms in the food chain [13].

Recent in situ investigations confirmed the interactions between the microplastics and heavy metals in the aquatic environment. The microplastics were found to contain metals such as Pb, Cd, Cu, Cr, Mn, Hg, Ni, and Zn along the coastline in many localities in different parts of the world [14-15]. Moreover, in Thailand, it is found that  $Cd^{2+}$  was accumulated on microplastics in the Chao Phraya River, with a concentration of  $2.81\pm2.05$  µg/g [16]. This study affirmed that

the microplastics could transfer heavy metal pollution from one location to another [17], and thus these copollutants can be transported through the food chain to humans [18]. Therefore, the implementation of heavy metal treatment in polluted water containing microplastics in the environment is of importance. There are various technologies used to treat heavy metals, such as dissolved air flotation, membrane filtration, coagulation, and ultrafiltration. However, these techniques often have high operating costs. Adsorption, on the other hand, is a low-cost wastewater technology that has been widely applied for heavy metal removal from polluted water [19]. In Thailand, bamboo biochar (BBC) and rice husk ash (RHA), byproducts of agricultural and biomass power plants, have emerged as promising adsorbents due to their porous structures, abundance, and low cost [20]. The present study aimed to explore the sorption mechanisms and adsorption capacities of cadmium on polypropylene (PP) microplastics, BBC, and RHA in aqueous solutions and possible transport behaviors of Cd2+ in the aquatic environment.

# **Materials and Methods**

Polypropylene (PP) particles from Merck Limited, Klongtoey, Bangkok (Thailand) were used in this study. The particles were sieved using U.S. mesh standard sieve numbers 50, 270 to obtain a particle size range of 0.05-0.30 mm [16]. To remove metal contaminants on the PP surface, the particles were rinsed with 0.1 M HCl, followed by washing with tap water and then distilled water. Virgin polypropylene particles were subsequently aged for 0, 1, 2, and 3 weeks, and denoted as PP<sub>0</sub>, PP<sub>1</sub>, PP<sub>2</sub>, and PP<sub>3</sub>, respectively. The aging process was conducted at 30±2°C to simulate the mechanical action of water flow. Ultraviolet A (UVA) lamps (4×18 W, with a wavelength range of 320-360 nm and a peak wavelength of 340 nm) were used to simulate sunlight UV irradiation. A shaker was operated at 200 rpm and 30±2°C to mimic river currents. The aging experiments were performed under a 12/12 h light/dark photoperiod. After aging, all samples were rinsed with deionized water (DI), dried in an oven at 60°C for 24 h, and stored in desiccators for further use.

Bamboo biochar (BBC) used in this study was produced in a Japanese kiln (Iwate kiln) at 1,000°C for 15 days from Bamboo D88, Nonthaburi (Thailand). Rice husk ash (RHA), a by-product obtained from a biomass power plant from Mungcharoen Green Power Co., Ltd., Surin (Thailand), was also used in this study. The power plant operates with high-pressure steam

at 65 bar and a combustion temperature of 480°C. Both BBC and RHA were sieved to obtain particle sizes from 0.25 to 1.0 mm using U.S. standard mesh sieve numbers 18 and 60. The samples were washed with DI until the pH value was equal to 7, dried at 60°C for 24 h in a hot air oven, and stored in desiccators for further use.

A solution of Cd<sup>2+</sup> was prepared using cadmium nitrate tetrahydrate (Cd(NO<sub>3</sub>)<sub>2</sub>·4H<sub>2</sub>O) of analytical grade from SD Fine-Chemical Limited (India). A stock solution with a concentration of 100 mg/L Cd<sup>2+</sup> was obtained by dissolving Cd(NO<sub>3</sub>)<sub>2</sub>·4H<sub>2</sub>O in DI. Working solutions of Cd<sup>2+</sup> with concentrations ranging from 1 to 10 mg/L were prepared by serial dilution of the stock solution with DI.

# Characterization of BBC, RHA, and PP

The surface morphologies of BBC, RHA, and PP were analyzed using a scanning electron microscope and energy dispersive spectroscopy (SEM-EDS, Phenom ProX, Thermo Fisher Scientific, US). The surface area, pore volume and pore diameter were measured using the Brunauer-Emmett-Teller (BET, Autosorb iQ-C-AG, Quantachrome Instrument, USA). The elemental compositions were determined using an X-ray fluorescence spectrometer (XRF, XUV 773, Fischer, Germany). The surface functional groups were characterized using Fourier-transform infrared spectroscopy (FTIR, Nicolet 6700, Thermo Scientific, USA). The physicochemical properties of the samples were evaluated to establish correlations between these properties and to elucidate the possible sorption mechanisms between the adsorbents and adsorbates.

The pH of the point of zero charge (pH<sub>PZC</sub>) of PP virgin (PP<sub>0</sub>), 1-week aged PP (PP<sub>1</sub>), 2-week aged PP (PP<sub>2</sub>), 3-week aged PP (PP<sub>3</sub>), BBC, and RHA was determined to investigate possible ion exchange properties of the adsorbents, which typically depend on the net surface charge. The method used for measuring the pH<sub>PZC</sub> was the solid addition method by using 45 mL of 0.1 M KNO3, and adjusting the pH values of each solution to 2.0-12.0 by using 0.1 N HNO<sub>3</sub> and 0.1 N NaOH, and adjusting the solution volume to 50 mL. Next, 1 g of each sample was added to separate containers. The solutions were agitated at 120 rpm in an incubator shaker for 48 h, and the final pH values of all samples were measured after 48 h. The initial pH on the x-axis versus the final pH on the y-axis was plotted to obtain the  $pH_{\mbox{\tiny PZC}}$  of each adsorbent. The intersecting point between these two lines is the  $pH_{PZC}$  [21, 22].

## Adsorption Kinetics and Isotherms

The adsorption kinetics of Cd<sup>2+</sup> onto PP<sub>0</sub>, PP<sub>1</sub>, PP<sub>2</sub>, PP<sub>3</sub>, BBC, and RHA were performed in volumetric flasks. A 100 mg/L Cd<sup>2+</sup> solution was diluted to a 1 mg/L stock solution. The total volume of each solution was 1000 mL. For the adsorption kinetic experiments, an initial Cd<sup>2+</sup> concentration of 1 mg/L

in 1000 mL solution was mixed with an adsorbent dosage of 4 g/L. The sorption experiments were operated at an agitation rate of 150 rpm at 30±2°C and an initial pH of  $7.0\pm0.1$ . The experiments were performed in duplicate. After the sorption kinetics, the samples were collected at 0, 5, 15, 30, 60, 120, 240, 480, 1140, 1440, and 2880 min, and filtered with 0.2 µm cellulose acetate syringe filters. Adsorption isotherms were studied using Cd2+ solutions with initial concentrations ranging from 1 to 10 mg/L, each placed in a 50-mL bottle with 0.2 g of adsorbent added. The equilibrium time obtained from adsorption kinetics was used for adsorption isotherm studies. The oscillator speed was set to 150 rpm at 30±2°C and an initial pH of 5.0. The Cd<sup>2+</sup> concentrations were analyzed with atomic absorption spectroscopy (AAS) (AA-6300, Shimadzu Corporation, Japan).

# Data Analysis

The adsorption kinetics of Cd<sup>2+</sup> were fitted using the pseudo-first-order (PFO) and pseudo-second-order (PSO) kinetic models, while the Langmuir and the Freundlich isotherm models were applied to fit the adsorption isotherm data. The corresponding model equations are shown in equations 1-4 [23]. These models were used to describe the adsorption mechanisms of cadmium onto PP<sub>0</sub>, PP<sub>1</sub>, PP<sub>2</sub>, PP<sub>3</sub>, BBC, and RHA.

$$\log(Q_e - Q_t) = \log Q_e - \frac{k_1}{2.303}t \tag{1}$$

$$\frac{t}{Q_t} = \frac{1}{k_2 Q_e^2} + \frac{1}{Q_e} t \tag{2}$$

$$\frac{1}{Q_e} = \frac{1}{Q_m} + \left(\frac{1}{Q_m K_L}\right) \frac{1}{C_e} \tag{3}$$

$$\log Q_e = \log K_F + \frac{1}{n} \log C_e \tag{4}$$

#### **Results and Discussion**

## Material Characterization

Fig. 1(a, b) shows SEM images of the morphology of PP<sub>0</sub> and PP<sub>3</sub>. The results indicate predominantly irregular surface morphologies. Their surface after magnification was rough and bumpy. A more irregular surface is generally associated with higher adsorption capacity [24]. Fig. 1(c, d) reveals pore sizes ranging from micropores to mesopores in BBC and RHA, with a honeycomb-like morphology and cylindrically shaped pores [25]. This structure suggests their potential application as absorbent materials. Table 1 presents the physical and chemical properties of PP<sub>0</sub>, BBC, and RHA. PP<sub>0</sub> and BBC showed high C content with relatively low Au and Si contents, whereas RHA exhibited

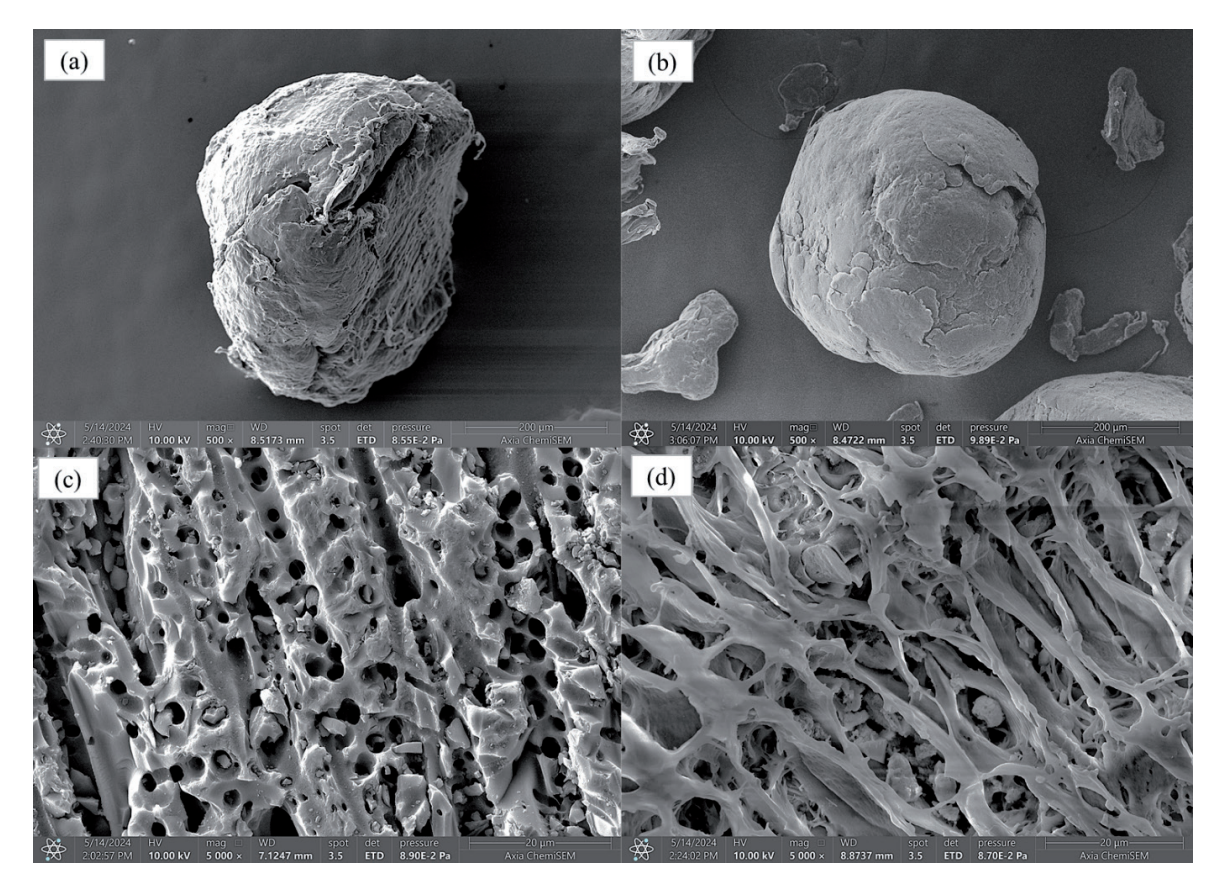


Fig. 1. SEM-EDS analysis of a) PP virgin, b) 3-week aged PP, c) BBC, and d) RHA.

a high Si content, appearing as mineral agglomerates on the fibers, along with a lower C content that reflects the structural characteristics typical of its biomass origin. In general, the presence of C, K, Mg, and Al is commonly observed in both biochar and microplastic [26, 27]. BET analysis revealed differences among PP<sub>o</sub>, BBC, and RHA. PP<sub>0</sub> exhibited the lowest surface area (2.422 m<sup>2</sup>/g), negligible pore volume of 0.0005 cm<sup>3</sup>/g, and a microporous structure (0.7848 nm), indicating a limited ability to provide active sites for Cd<sup>2+</sup> sorption. In contrast, BBC demonstrated the highest surface area  $(136.016 \text{ m}^2/\text{g})$  and pore volume  $(0.0387 \text{ cm}^3/\text{g})$ , with a mesoporous structure (3.0105 nm), suggesting strong potential for ion diffusion and adsorption. RHA also exhibited a relatively high surface area (103.051 m<sup>2</sup>/g), with an average pore diameter of 2.7369 nm, reflecting its silica-rich and porous nature. Pore-size

distribution analysis revealed that both BBC and RHA are predominantly mesoporous (2-50 nm), while PP is largely microporous (<2 nm) [28]. These findings suggest that BBC, RHA, and PP can be considered effective adsorbents for pollutants, with BBC showing the highest performance [29].

XRF analysis revealed that PP<sub>0</sub> primarily contained P<sub>2</sub>O<sub>5</sub> (10.7%) and Fe<sub>2</sub>O<sub>3</sub> (10.6%), suggesting a considerable contribution of phosphate and iron-based mineral phases to the surface chemistry of the material. The high concentration of P<sub>2</sub>O<sub>5</sub> implies that phosphate functionalities provide negatively charged site groups. These groups act as strong ligands capable of complexing with divalent and trivalent metal cations (Cd<sup>2+</sup>, Pb<sup>2+</sup>, Fe<sup>3+</sup>) via inner-sphere complexation mechanisms [30]. Moreover, Fe-oxide surfaces carry amphoteric Fe–OH group exhibit pH dependent charges

Table 1. Physical and chemical properties of PP<sub>0</sub>, BBC, and RHA.

Sample	BET surface area (m <sup>2</sup> /g)	Pore volume (cm³/g)	Average pore diameter (nm)	Elemental composition (% w/w)						
				С	Si	Au	О	K	Mg	Al
$PP_0$	2.422	0.0005	0.7848	98.4	0.1	1.5	ND	ND	ND	ND
BBC	136.016	0.0387	3.0105	99.3	0.2	0.5	ND	ND	ND	ND
RHA	103.051	0.0373	2.7369	7.1	36.6	ND	53.6	4.4	0.3	0.3

ND: not detected

(PZC typically near neutral), enabling them to either attract Cd<sup>2+</sup> electrostatically (as Fe-O<sup>-</sup> above the PZC) or competition with co-adsorbing anions [31], while BBC was dominated by K<sub>2</sub>O (67.7%) along with CaO (8.33%), Na<sub>2</sub>O (5.40%) and MgO (2.42%). This alkali (K, Na) and alkaline earth metals (Ca, Mg) tend to release positively charged cations (K+, Na+, Ca2+, Mg2+) upon hydration, which can associate with surface oxygen-containing groups and shift the surface charge toward positive [32] and RHA by SiO, (83.5%) which would usually suggest a negative surface charge due to the presence of deprotonated silanol groups. However, the presence of K<sub>2</sub>O (5.44%), CaO (3.46%), and MgO (0.86%), although at lower concentrations than in BBC, can still contribute positively charged species that may neutralize or overcome the negative charges from Si-OH, particularly in acidic to neutral pH conditions [33]. The presence of these chemical components is likely to influence the sorption of Cd2+ onto the adsorbents through surface chemical interactions.

The adsorption behavior is influenced by the chemical reactivity of the surface, especially in the form of chemisorbed oxygen in various forms of functional groups. FTIR shows results as Fig. 2, several peaks had disappeared at 3600-3200 cm<sup>-1</sup> (O-H stretching vibrations of hydrogen-bonded hydroxyl groups and water). The peak at 3415 cm<sup>-1</sup> was attributed to the presence of the O-H functional group (alcoholic and phenolic) and water. The surface complexation adsorption is great for -COOH and -OH functional groups, such as those in alcohols, phenols, or carboxyl. These groups are active sites for surface complexation with cations as Cd<sup>2+</sup> [34]. However, RHA has the peak of Si-O-Si stretching at 1093.97 cm<sup>-1</sup>, consistent with its high SiO, content. This may also affect the sorption mechanism by providing reactive oxygencontaining sites [35]. These play a guiding role in the adsorption mechanism of Cd<sup>2+</sup> by biochar in surface water [36].

The pH<sub>PZC</sub> values obtained for PP<sub>0</sub> (6.4), PP<sub>1</sub> (5.2), PP<sub>2</sub> (4.9), PP<sub>3</sub> (4.7), BBC (8.0), and RHA (9.7). Given that the pH of the solution applied in this study was approximately 7.0±0.1, the surfaces of all adsorbents would be negatively charged, promoting electrostatic attraction toward cations such as Cd<sup>2+</sup>. PP<sub>0</sub> and PP<sub>1</sub>, with pH<sub>PZC</sub> slightly below the solution pH, likely generate moderate negative surface charges; PP, and PP, with even lower pH<sub>PZC</sub> values, would exhibit stronger negative charge, thus potentially enhancing their cation adsorption efficacy. The BBC and RHA have relatively high pH<sub>PZC</sub> values, which might indicate that their surfaces would be positively charged at neutral pH. However, their surfaces often contain abundant oxygencontaining functional groups that can deprotonate and generate negative surface charges even below the pH<sub>pzc</sub> [31]. This surface chemistry enables Cd<sup>2+</sup> adsorption via surface complexation and ion exchange, which can override the purely electrostatic behavior predicted from pH<sub>PZC</sub> alone. The relatively high pH<sub>PZC</sub> values of BBC and RHA are attributed to their alkaline mineral composition, notably K<sub>2</sub>O, CaO, and MgO, which contributes to basic surface sites [33].

Characterization confirmed the role of physicochemical properties in adsorption. SEM-EDS showed surface roughness and morphological changes, BET revealed differences in surface area and porosity linked to adsorption capacity, XRF identified residual minerals influencing surface charge, and FTIR detected oxygen-containing functional groups as active Cd<sup>2+</sup> binding sites. Together, these analyses establish the mechanistic link between surface chemistry, porosity, and sorption performance [32].

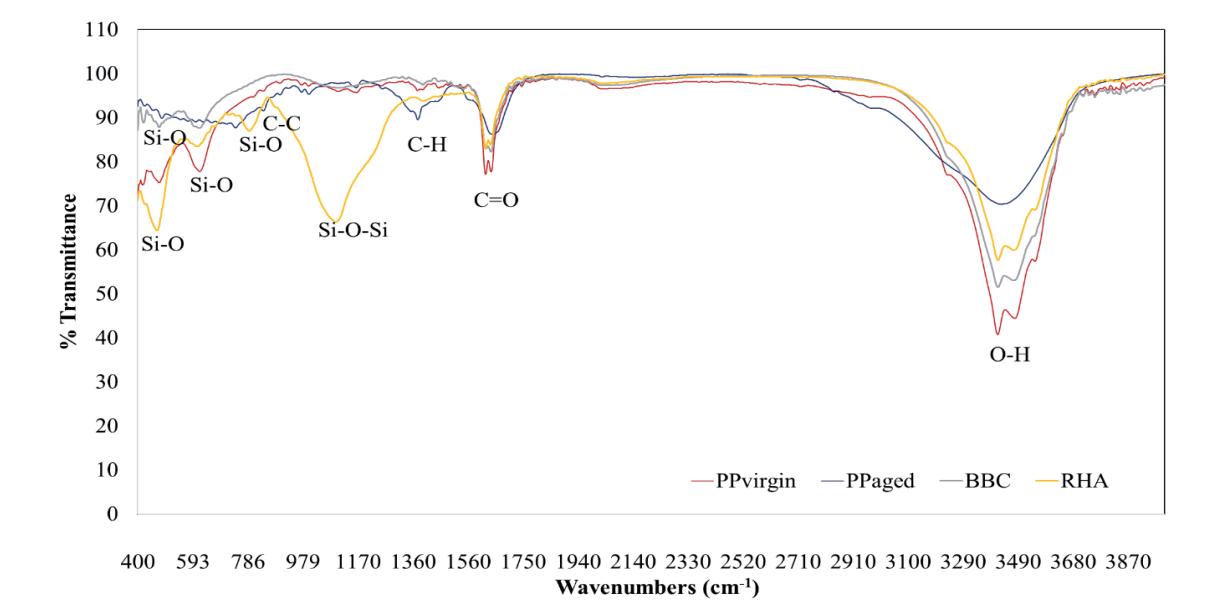


Fig. 2. FTIR analysis of virgin PP, 3-week aged PP, BBC, and RHA.

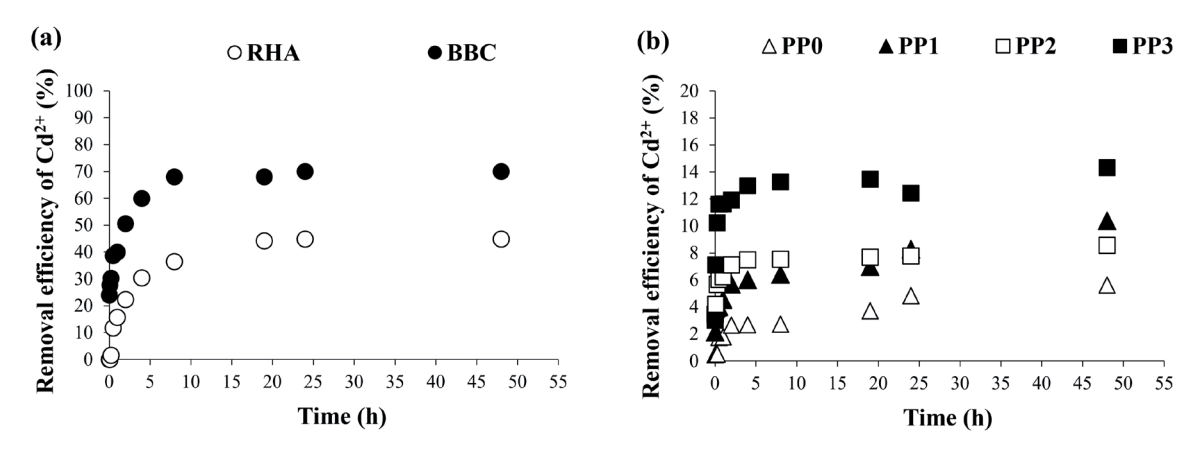


Fig. 3. Effect of contact time on the removal efficiencies of Cd2+ by a) BBC and RHA, and by b) PP0-PP2.

# Adsorption Kinetics

The adsorption kinetics are performed to investigate the effect of contact time on the sorption capacity of Cd<sup>2+</sup> onto the PP<sub>0</sub>-PP<sub>3</sub>, BBC, and RHA. The results are presented in Fig. 3. PP<sub>0</sub>-PP<sub>3</sub> reached the equilibrium time at a similar period around 1140 min, and PP<sub>3</sub> had the highest removal efficiency for Cd<sup>2+</sup>. The aging of PP affected its ability to adsorb more Cd<sup>2+</sup>, with longer aging times resulting in higher Cd<sup>2+</sup> binding capacity. The increased Cd<sup>2+</sup> adsorption on PP aged can be attributed to the surface oxidation that occurs during the aging process. The oxygen-containing functional

groups that are produced provide sorption sites and thus enhance the adsorption capacity of metal ions [37]. The BBC and RHA reached equilibrium times at a similar time, around 1140 min, and the BBC had a higher removal efficiency for Cd<sup>2+</sup> than RHA. This can be due to the smaller surface area and pore volume of BBC than RHA, which can attract more cations to adsorb on the surface.

Sorption model fitting by PFO and PSO is shown in Fig. 4 and Fig. 5, respectively. The adsorption kinetics are summarized in Table 2. The R<sup>2</sup> value could reflect the goodness of fit of each model. The R<sup>2</sup> values for PP<sub>0</sub>-PP<sub>3</sub>, BBC, and RHA using the PFO model were

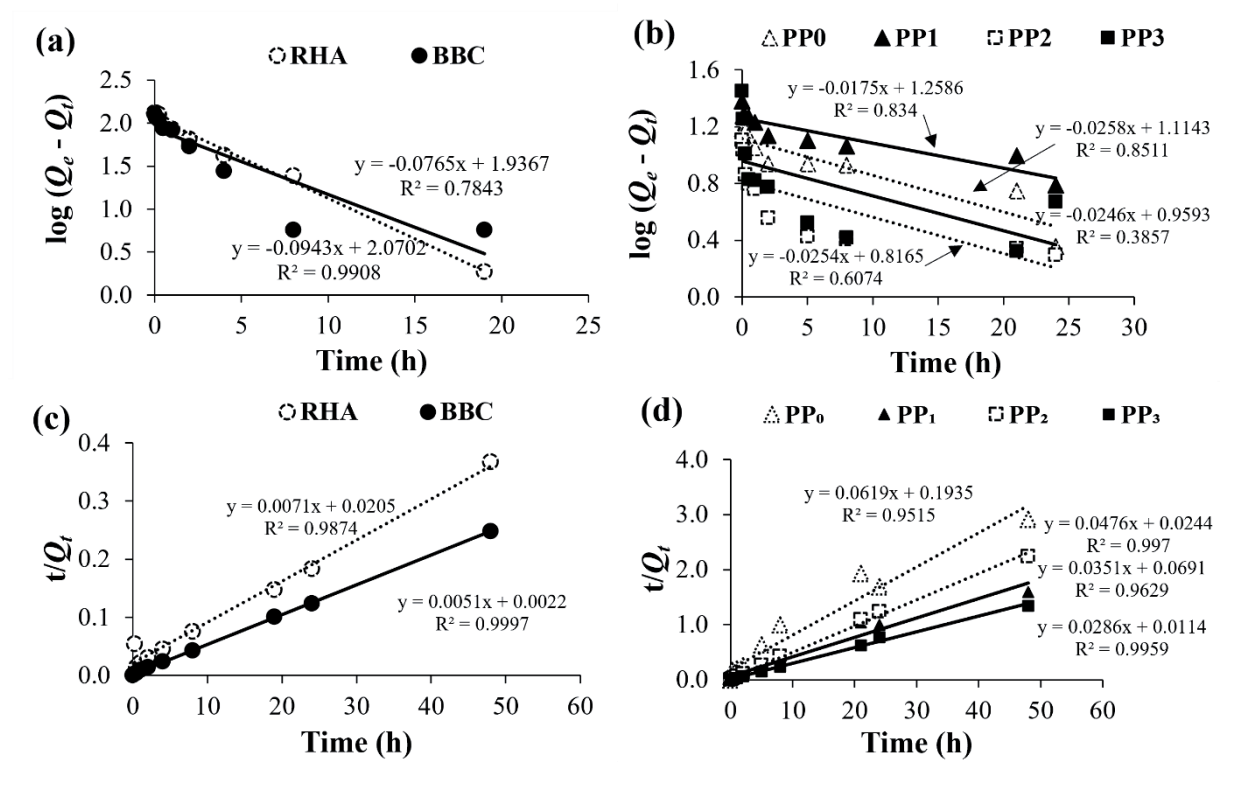


Fig. 4. Linear fittings of PFO kinetics for a) BBC and RHA and for b) PP (PP<sub>0</sub>-PP<sub>3</sub>), and PSO kinetics for c) BBC and RHA and for d) PP (PP<sub>0</sub>-PP<sub>3</sub>).

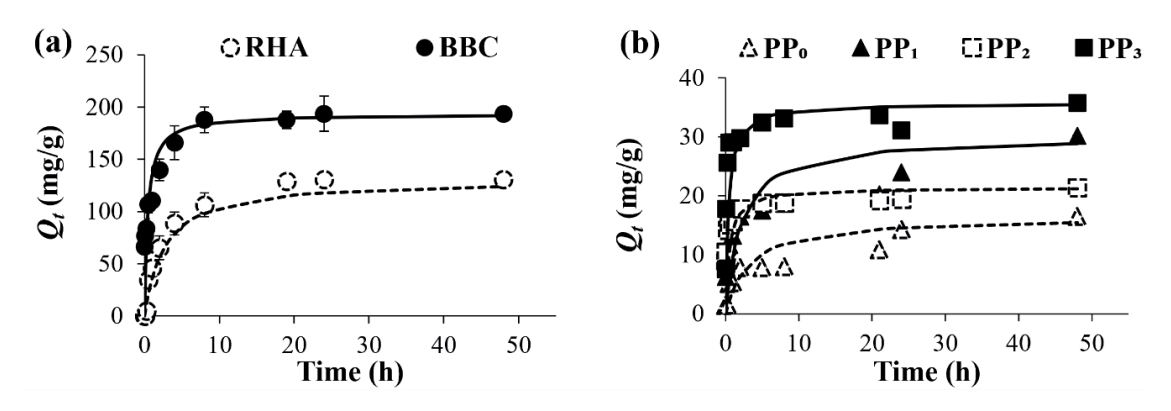


Fig. 5. Non-linear PSO model fittings for a) BBC and RHA, and for b) virgin PP (PP<sub>0</sub>) and aged PP (PP1-PP<sub>3</sub>).

Table 2. Adsorption kinetic constants of PFO and PSO models, and adsorption isotherm constants of Langmuir and Freundlich models.

Sample	Kinetic models						Isotherm models						
	PFO			PSO			Langmuir			Freundlich			
	(1/min)	$Q_e \pmod{\mathrm{mg/g}}$	$R^2$	K <sub>2</sub> (g/mg min)	$Q_e \pmod{\mathrm{mg/g}}$	$R^2$	<i>K<sub>L</sub></i> (1/min)	$Q_m$ (mg/g)	$R^2$	K <sub>F</sub> (g/mg min)	n (mg/g)	$R^2$	
$PP_0$	0.059	13.01	0.851	0.019	16.16	0.951	0.267	345.26	0.972	67.639	1.51	0.987	
$PP_1$	0.040	18.14	0.834	0.016	28.50	0.963	0.237	400.99	0.974	71.276	1.44	0.987	
$PP_2$	0.059	6.55	0.607	0.090	21.00	0.997	0.162	550.17	0.827	74.573	1.41	0.997	
PP <sub>3</sub>	0.057	9.11	0.385	0.069	34.97	0.996	0.146	633.89	0.770	78.866	1.38	0.996	
BBC	0.176	86.45	0.784	0.012	195.28	0.999	0.635	779.47	0.831	291.163	2.58	0.884	
RHA	0.217	117.54	0.990	0.003	141.40	0.987	0.805	815.02	0.959	320.778	2.57	0.903	

0.851, 0.834, 0.607, 0.385, 0.784, and 0.990, respectively. In contrast, the PSO model provided higher  $R^2$  values of 0.951, 0.963, 0.997, 0.996, 0.999, and 0.987, respectively. The  $Cd^{2+}$  sorption data conform better to the PSO model, with  $R^2$  were limited to unity.

PP<sub>0</sub>-PP<sub>2</sub> and BBC exhibited a better fit with the PSO model than the PFO model, implying that chemisorption, likely involving surface complexation with oxygen-containing functional groups, the dominant mechanism. The sorption kinetics of Cd<sup>2+</sup> on PP at different aging stages were best described by the PSO model, indicating chemisorption is the dominant mechanism. The increased R<sup>2</sup> values with extended aging suggest enhanced chemical interaction between Cd<sup>2+</sup> and the PP surface, likely due to surface oxidation, enhanced roughness and porosity, and the generation of oxygen-containing functional groups (-COOH, -OH), which serve as active binding sites. These findings are in agreement with Wang et al. (2024) [38], who reported that the adsorption of Cd2+ onto UV-aged polystyrene microplastics and biochar also followed pseudosecond-order kinetics more closely ( $R^2 = 0.8642$ ) than the pseudo-first-order model ( $R^2 = 0.7711$ ), suggesting that chemical adsorption is a key process in Cd<sup>2+</sup> retention on both synthetic and biomass-derived sorbents. Feng et al. (2025) [39] reported a 22-27% increase in Cd<sup>2+</sup> adsorption on aged microplastics due to greater surface area and functional group availability. The present study supports these mechanisms. Notably, the highest R<sup>2</sup> value (0.997) was observed for PP aged for 2 weeks, indicating optimal surface modification. In contrast, the comparable R<sup>2</sup> values observed at 3 weeks (0.996-0.999) may reflect a plateau effect, suggesting that beyond a certain aging duration, the adsorption performance stabilizes with minimal further improvement.

Conversely, RHA provided a better fit with the PFO model ( $R^2 = 0.990$ ), suggesting that physical adsorption was the dominant mechanism. This observation aligns closely with findings by Nnaji et al. (2017), who demonstrated that RHA adsorption kinetics for Pb2+ were well described by PFO ( $R^2 = 0.987$ ), with ion exchange being a dominant removal mechanism under acidic to neutral pH [40]. Collectively, the contrasting kinetic behaviors emphasize the role of surface chemistry and porosity characteristics in governing metal uptake: while biomass-derived adsorbents may follow chemisorption pathways, RHA appears to rely more on physisorption under certain conditions. Nevertheless, PP, BBC, and RHA have a good fitting effect, suggesting that partial complexation and chemical adsorption may control the whole adsorption process [41].

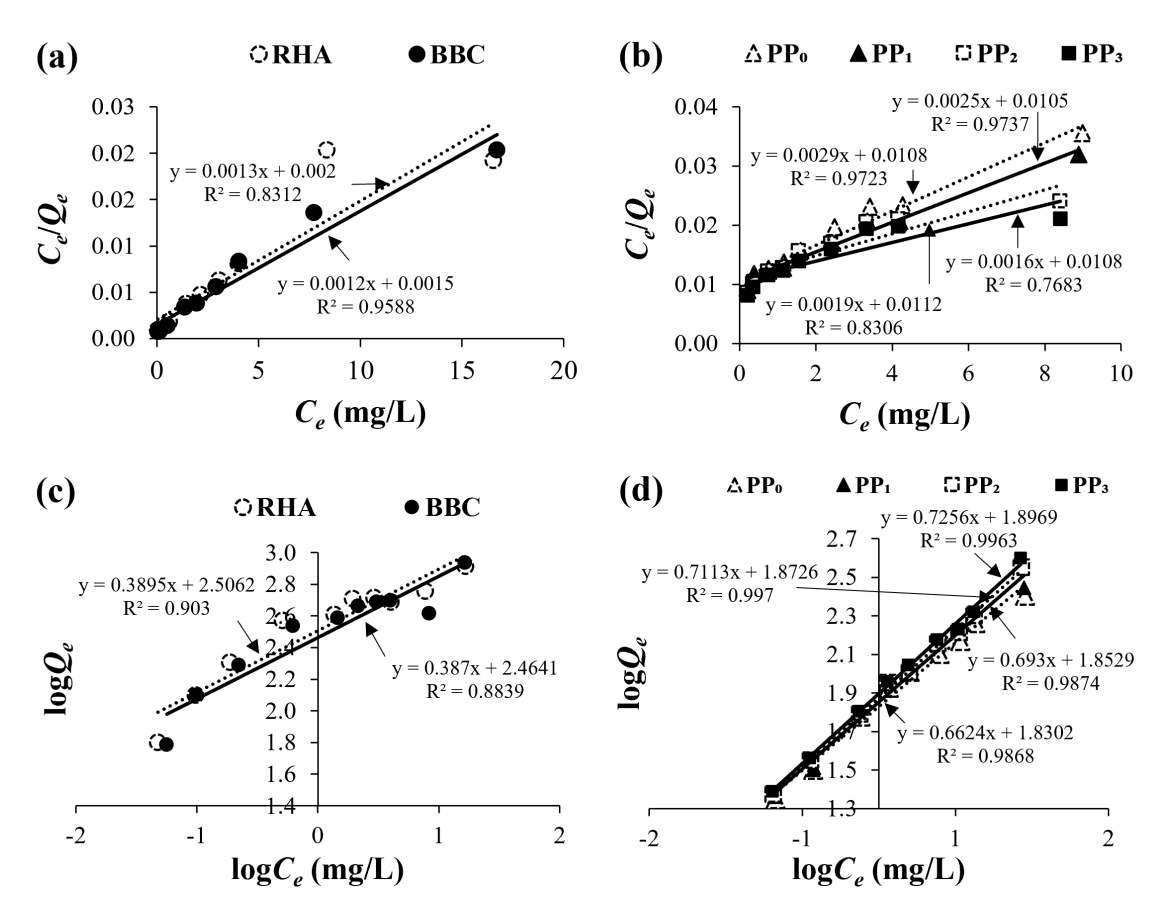


Fig. 6. Linear fittings of Langmuir isotherms for a) BBC and RHA and for b) PP  $(PP_0-PP_3)$ , and Freundlich isotherms for c) BBC and RHA and for d) PP  $(PP_0-PP_3)$ .

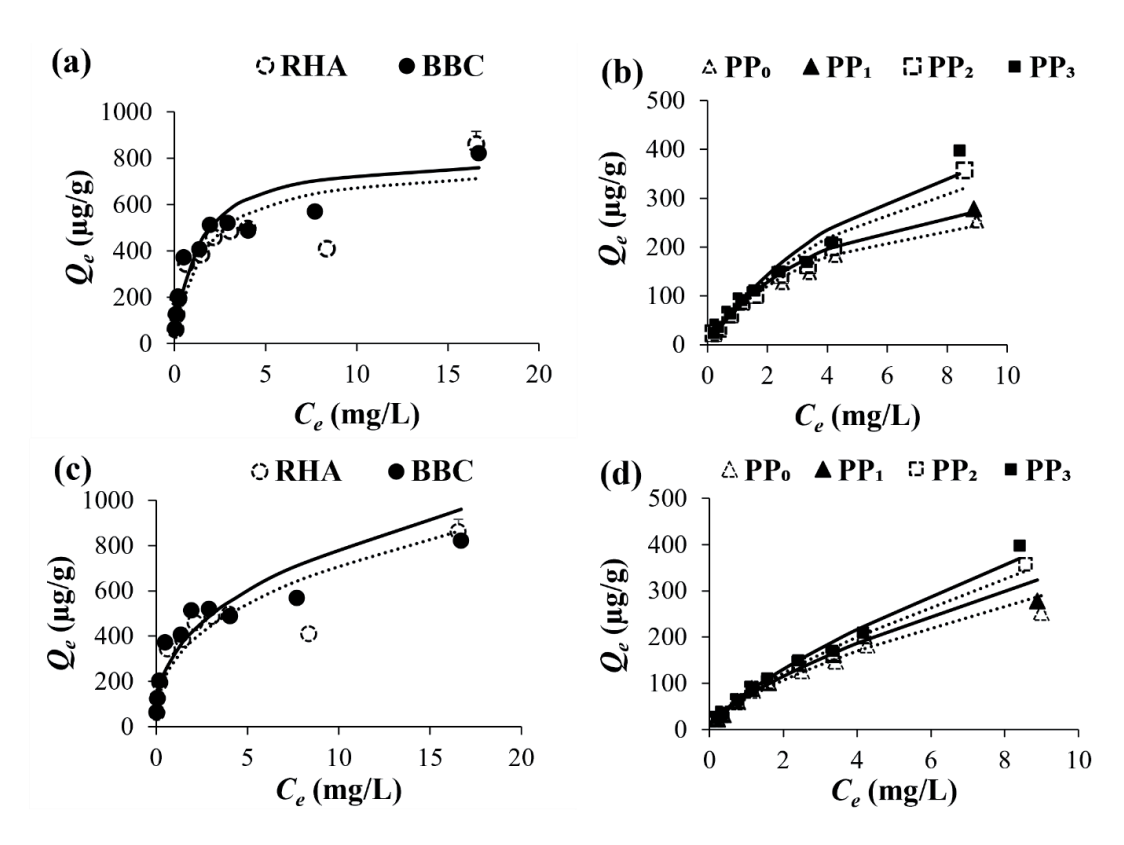


Fig. 7 Non-linear fittings of Langmuir isotherms for a) BBC and RHA and for b) PP (PP<sub>0</sub>-PP<sub>3</sub>), and Freundlich isotherms for c) BBC and RHA and for d) PP (PP<sub>0</sub>-PP<sub>3</sub>).

#### Adsorption Isotherms

The Freundlich model and the Langmuir model are capable of effectively fitting the adsorption behavior of  $PP_0$ - $PP_3$ , BBC, and RHA to  $Cd^{2+}$ . The correlation coefficients explaining the adsorption equilibrium mechanisms involved in each model are presented in Fig. 7. The  $PP_0$ - $PP_3$  and BBC samples were better fit with the Freundlich isotherm model, with  $R^2$  values of 0.987, 0.987, 0.997, 0.996, and 0.884, respectively. This suggests that the adsorption process occurs on a heterogeneous surface with varying affinities for  $Cd^{2+}$  ions, indicating multilayer adsorption. In contrast, the RHA was a better fit with the Langmuir isotherm model,  $R^2 = 0.959$ , suggesting monolayer adsorption on a homogeneous surface [42].

The adsorption equilibrium was effectively described by both the Langmuir and the Freundlich isotherm models. However, the Freundlich model showed higher correlation coefficients, particularly for PP<sub>0</sub>-PP<sub>2</sub> and BBC, indicating multilayer adsorption on heterogeneous surfaces [43]. This behavior is likely attributed to the presence of oxygen-containing functional groups and diverse sorption sites resulting from environmental aging and pyrolysis processes. These findings are consistent with Muthuraja et al. (2021) [44], who demonstrated that aged microplastics and biochar exhibited Freundlich-type Cd2+ adsorption due to their heterogeneous surface chemistry and mechanisms such as surface complexation and electrostatic attraction [45]. Similarly, Simón et al. (2024) [46] reported that biochar from agricultural waste follows the Freundlich model, influenced by microporous structures and functional group diversity. Alves et al. (2021) [47] also found that Freundlich isotherms better fit Cd2+ adsorption on modified biomass adsorbents, supporting the presence of multilayer chemisorption. In contrast, the Langmuir model provided a better fit for RHA, suggesting monolayer adsorption on a more homogeneous and silica-rich surface.

The overall isotherm parameters imply that Cd<sup>2+</sup> adsorption across all tested materials is predominantly chemical in nature. This interpretation is further supported by Wang et al. (2024) [38], who demonstrated that multilayer adsorption coupled with pseudo-second-order kinetics is indicative of chemisorption involving ion exchange and specific interactions at the adsorbent surface.

The kinetic and isotherm model interpretations are consistent with the characterization results, providing clearer insights into the specific mechanisms driving Cd<sup>2+</sup> adsorption on the different adsorbents.

### **Conclusions**

This study investigated the sorption behaviors and mechanisms of  $Cd^{2+}$  on virgin and aged PP (PP<sub>0</sub>, PP<sub>1</sub>, PP<sub>2</sub>, and PP<sub>3</sub>), BBC, and RHA. Characterization

results revealed that differences in surface morphology, functional groups, and porosity directly influenced adsorption mechanisms, which suggests a good adsorption removal capacity.

The removal efficiencies of Cd2+, with initial Cd2+ concentration of 1 mg/L, by PP<sub>0</sub>, PP<sub>1</sub>, PP<sub>2</sub>, PP<sub>3</sub>, BBC and RHA were 5.62%, 10.39%, 8.56%, 14.31%, 70.03%, and 44.78%, respectively, under the optimum adsorption conditions at pH 7.0, temperature of 25°C, at adsorbent dosage of 4.0 g/L and in adsorption time of 1140 min. The PP3 exhibited the highest removal efficiency for Cd2+. However, the aging of PP affected its ability to adsorb more Cd2+, with longer aging times resulting in a higher capacity to bind with Cd<sup>2+</sup>. The sorption models of kinetics and isotherms were used to fit the experimental results; PSO models fitted the data better than PFO for all of PP and BBC. Thus, the excellent PSO model fit across aged PP samples, especially from week 2 onward, confirms that chemical interactions dominate the sorption process, and this behavior is significantly promoted by aging-induced surface modifications. This suggested that the sorption of Cd<sup>2+</sup> may imply chemical bond formation and ion exchange, consistent with Muthuraja et al. (2021) [44]. RHA is a better fit with the PFO model, suggesting that physisorption on its silica-rich surface, as also noted by Wang et al. (2024) [38]. The Freundlich isotherm model best fitted the results for PP and BBC, with maximum adsorption capacities of 396.7 µg/g and 862.6 µg/g, respectively. These imply a formed multilayer adsorption on heterogeneous surfaces. In contrast, for RHA, the fit of the Langmuir isotherm model was better, with a maximum adsorption capacity of 758.63 µg/g. It indicates that the monolayer sorption mechanism dominated the experiments. The characteristic analysis and modeling results suggested that multiple mechanisms might control the Cd<sup>2+</sup> sorption, such as intraparticle diffusion and functional groups on the surface serving as sorption sites for the cations of toxic metals [34].

This study provides a comparative evaluation of aged polypropylene microplastics and biomass-derived adsorbents, demonstrating how environmental aging alters plastic surface properties and influences their interaction with heavy metals. The results confirm the superior performance of agricultural waste-based adsorbents in removing Cd<sup>2+</sup> and highlight the emerging environmental risks associated with co-contamination by aged microplastics and heavy metals in aquatic systems. [48].

## Acknowledgements

The authors are very grateful to the Environment Technology Program, School of Energy, Environment and Materials (SEEM), for supporting the research work. This research was supported by King Mongkut's University of Technology Thonburi (KMUTT), Thailand Science Research and Innovation (TSRI), and National

Science, Research and Innovation Fund (NSRF) Fiscal year 2024 Grant number FRB670016/0164, and the King Mongkut's University of Technology Thonburi fund (fiscal year 2020).

#### **Conflict of Interest**

The authors declare no conflicts of interest.

# References

- WANG M., CHEN Z., SONG W., HONG D., HUANG L., LI Y. A review on cadmium exposure in the population and intervention strategies against cadmium toxicity. Bulletin of Environmental Contamination and Toxicology. 106 (1), 65, 2021.
- SALL M.L., DIAW A.K.D., GNINGUE-SALL D., EFREMOVA AARON S., AARON J.J. Toxic heavy metals: impact on the environment and human health, and treatment with conducting organic polymers, a review. Environmental Science and Pollution Research. 27 (24), 29927, 2020.
- 3. ASOKBUNYARAT V., SIRIVITHAYAPAKORN S. Heavy metals in sediments and water at the Chao Phraya River mouth, Thailand. Thai Environmental Engineering Journal. 34, 33, 2020.
- MINISTRY OF SCIENCE, TECHNOLOGY AND ENVIRONMENT. Notification of the Ministry of Science, Technology and Environment No. 8: Surface water quality standards, B.E. 2537 (1994). Bangkok, Thailand, 1994.
- WANG J., PENG J., TAN Z., GAO Y., ZHAN Z., CHEN Q., LIQI C. Microplastics in the surface sediments from the Beijiang River littoral zone: composition, abundance, surface textures and interaction with heavy metals. Chemosphere. 171, 248, 2017.
- YANG L., ZHANG Y., KANG S., WANG Z., WU C. Microplastics in soil: A review on methods, occurrence, sources, and potential risk. Science of The Total Environment. 780, 146546, 2021.
- ERIKSEN M., LEBRETON L.C., CARSON H.S., THIEL M., MOORE C.J., BORERRO J.C., GALGANI F., RYAN P.G., REISSER J. Plastic pollution in the world's oceans: more than 5 trillion plastic pieces weighing over 250,000 tons afloat at sea. PLoS One. 9 (12), e111913, 2014.
- NAQASH N., PRAKASH S., KAPOOR D., SINGH R. Interaction of freshwater microplastics with biota and heavy metals: a review. Environmental Chemistry Letters. 18 (6), 1813, 2020.
- AMELIA T.S.M., KHALIK W.M.A.W.M., ONG M.C., SHAO Y.T., PAN H.J., BHUBALAN K. Marine microplastics as vectors of major ocean pollutants and its hazards to the marine ecosystem and humans. Progress in Earth and Planetary Science. 8, 12, 2021.
- GEYER R. Production, use, and fate of synthetic polymers. Plastic Waste and Recycling. 13, 2020.
- 11. THUSHARI G.G.N., SENEVIRATHNA J.D.M. Plastic pollution in the marine environment. Heliyon. 6 (8), e04709, 2020.
- 12. MATOS M.D., RAMOS J.A., BRANDAO A.L.C., BAETA A., RODRIGUES I., SANTOS I., COENTRO D.J., FERNANDES J.O., BATISTA DE CARVALHO L.A.E., MARQUES M.P.M., CUNHA S.C., SANTOS

- S.H., ANTUNES S., SILVA V., PAIVA V.H. Microplastics ingestion and endocrine disrupting chemicals (EDCs) by breeding seabirds in the east tropical Atlantic: Associations with trophic and foraging proxies ( $\delta^{15}$ N and  $\delta^{13}$ C). Science of The Total Environment. **912**, 168664, **2024**.
- SHEN M., SONG B., ZENG G., ZENG Y., TENG F., ZHOU C. Surfactant changes lead adsorption behaviors and mechanisms on microplastics. Chemical Engineering Journal. 405, 126989, 2021.
- 14. DOBARADARAN S., SCHMIDT T.C., NABIPOUR I., KHAJEAHMADI N., TAJBAKHSH S., SAEEDI R., JAVAD MOHAMMADI M., KESHTKAR M., KHORSAND M., FARAJI GHASEMI F. Characterization of plastic debris and association of metals with microplastics in coastline sediment along the Persian Gulf. Waste Management. 78, 649, 2018.
- 15. MIKHAILENKO A.V., RUBAN D.A. Plastics and Five Heavy Metals from Sea Beaches: A Geographical Synthesis of the Literary Information. Journal of Marine Science and Engineering. 11 (3), 626, 2023.
- TA A.T., BABEL S. Microplastics pollution with heavy metals in the aquaculture zone of the Chao Phraya River Estuary, Thailand. Marine Pollution Bulletin. 161, 111747, 2020.
- 17. KEDZIERSKI M., D'ALMEIDA M., MAGUERESSE A., LE GRAND A., DUVAL H., CESAR G., SIRE O., BRUZAUD S., LE TILLY V. Threat of plastic ageing in marine environment. Adsorption/desorption of micropollutants. Marine Pollution Bulletin. 127, 684, 2018.
- 18. DING C., CHEN J., ZHU F., CHAI L., LIN Z., ZHANG K., SHI Y. Biological toxicity of heavy metal(loid)s in natural environments: From microbes to humans. Frontiers in Environmental Science. 10, 920957, 2022.
- TONG M., HE L., RONG H., LI M., KIM H. Transport behaviors of plastic particles in saturated quartz sand without and with biochar/Fe<sub>3</sub>O<sub>4</sub>-biochar amendment. Water Research. 169, 115284, 2020.
- AKHTAR M., SARFRAZ M., AHMAD M., RAZA N., ZHANG L., Use of low-cost adsorbent for waste water treatment: Recent progress, new trend and future perspectives, Desalination and Water Treatment. 321, 100914, 2025.
- KHANDAKER S., TOYOHARA Y., KAMIDA S., KUBA T. Adsorptive removal of cesium from aqueous solution using oxidized bamboo charcoal. Water Resource and Industry. 19, 35, 2018.
- 22. JAWAD A.H., MALEK N.N.A., ABDULHAMEED A.S., RAZUAN R. Synthesis of magnetic chitosan-fly ash/ Fe<sub>3</sub>O<sub>4</sub> composite for adsorption of reactive orange 16 dye: optimization by Box–Behnken design. Journal of Polymers and the Environment. 28 (3), 1068, 2020.
- REVELLAME E.D., FORTELA D.L., SHARP W., HERNANDEZ R., ZAPPI M.E. Adsorption kinetic modeling using pseudo-first order and pseudo-second order rate laws: A review. Cleaner Engineering and Technology. 1, 100032, 2020.
- 24. RAZANAJATOVO R.M., DING J., ZHANG S., JIANG H., ZOU H. Sorption and desorption of selected pharmaceuticals by polyethylene microplastics. Marine Pollution Bulletin. 136, 516, 2018.
- FARHANA A.N., ALIAS A.B., TALIB N., RASHID Z., GHANI W.A.W.A.K. Characteristics of rice husk biochar blended with coal fly ash for potential sorption material. Malaysian Journal of Analytical Sciences. 22 (2), 326, 2018.

- 26. BOUREGBA R., BOUIADJRA B.A.B., BOUZIANE M.M., BELLALI M.A., SALEM M. Effect of thermal ageing on the thermal and mechanical properties of polypropylene and polypropylene micro-composites. Journal of Polymer Materials. 41 (3), 143, 2024.
- 27. CAÑON-TAFUR L.A., MATEUS-MALDONADO J.F., LOZANO-PUENTES H.S., HERRERA-ACOSTA C.D., SÁNCHEZ-MATIZ J.J., DÍAZ-ARIZA L.A., COSTA G.M., JIMÉNEZ-BORREGO L.C., CARRASCAL-CAMACHO A.K., PEDROZA-RODRÍGUEZ A.M. Guadua angustifolia biochar/TiO<sub>2</sub> composite and biochar as bio-based materials with environmental and agricultural applications. Scientific Reports. 15 (1), 246, 2025.
- 28. SEIFI S., LEVACHER D., RAZAKAMANANTSOA A.R., SEBAIBI N. Microstructure of dry mortars without cement: specific surface area, pore size and volume distribution analysis. Applied Sciences. 13 (9), 5616, 2023.
- 29. MELÉNDEZ F.M., SEGURA-CHAVARRÍA D., GARCÍA-GONZÁLEZ C.A., QUESADA-KIMSEY J., VILLAGRA K. Variability of Physical and Chemical Properties of TLUD Stove Derived Biochars. Applied Sciences. 10 (2), 507, 2020.
- QIU C., WANG C., LIU Q., GAO M., SONG Z. Effective removal of Cd from aqueous solutions using P-loaded Ca-Mn-impregnated biochar. Molecules. 28 (22), 7553, 2023.
- KOSMULSKI M. The pH dependent surface charging and points of zero charge. X. Update. Advances in Colloid and Interface Science. 319, 102973, 2023.
- 32. LIU Z., XU Z., XU L., BUYONG F., TAY C.C., LI Z., CAI Y., HU B., ZHU Y., WANG X. Modifed biochar: synthesis and mechanism for removal of environmental heavy metals. Carbon Research. 1, 8, 2022.
- 33. BOLAN N., SARMAH A.K., BORDOLOI S., BOLAN S., PADHYE L.P., VAN ZWIETEN L., SOORIYAKUMAR P., KHAN B.A., AHMAD M., SOLAIMAN Z.M., RINKLEBE J., WANG H., SINGH B.P., SIDDIQUE K.H.M. Soil acidification and the liming potential of biochar. Environmental Pollution. 317, 120632, 2023.
- 34. ALUTHGE M.D., WEERASINGHE A.S., WICKRAMASINGHE U.M., KULASEKARA B.R., KUMARASIRI L.M., COORAY A.T., RAJAPAKSHA S.P., VITHANAGE M. Sugarcane biomass-derived biochar for soil quality enhancement in sugarcane-growing soil. Carbon Research. 4, 9, 2025.
- 35. NGUYEN T.A., PHAN P.T., NGUYEN N.H., NGUYEN T.T. Rice husk ash as a great potential adsorbent in multipurpose adsorption of various pollutants: A review. Egyptian Journal of Chemistry. 66 (11), 1, 2023.
- 36. GUO Y., TAN C., SUN J., LI W., ZHANG J., ZHAO C. Porous activated carbons derived from waste sugarcane bagasse for CO<sub>2</sub> adsorption. Chemical Engineering Journal. 381, 122736, 2019.

- 37. HOTOVÁ G., SLOVÁK V., ZELENKA T., MARŠÁLEK R., PARCHAŇSKÁ A. The role of the oxygen functional groups in adsorption of copper (II) on carbon surface. Science of The Total Environment. 711, 135436, 2020.
- WANG M., JIANG X., WEI Z., WANG L., SONG J., CEN P. Enhanced cadmium adsorption dynamics in water and soil by polystyrene microplastics and biochar. Nanomaterials. 14 (13), 1067, 2024.
- 39. FENG F., WANG S., HE X., WANG X., HUANG J., LIU G., RONG S., SU S., YAN H., HAN B., LIU W. Adsorption behavior and mechanism of cadmium, copper, and lead on polylactic acid microplastics exposed to ultraviolet light. Journal of Environmental Chemical Engineering. 13 (3), 117033, 2025.
- 40. NNAJI C.C., EBEAGWU C.J., UGWU E.I. Physicochemical conditions for adsorption of lead from water by rice husk ash. Bio Resources. 12 (1), 799, 2017.
- 41. PINTOR A., VIEIRA B., BRANDÃO C.C., BOAVENTURA R.A.R., BOTELHO C.M.S. Complexation mechanisms in arsenic and phosphorus adsorption onto iron-coated cork granulates. Journal of Environmental Chemical Engineering. 8 (5), 104184, 2020.
- 42. KALAM S., ABU-KHAMSIN S.A., KAMAL S.M., PATIL S. Surfactant Adsorption Isotherms: A Review. ACS Omega. 6 (48), 32342, 2021.
- 43. LIU J., GAO X., WU X., ZHANG Z., ZHANG X. Sorption of cadmium by rice husk char, bamboo char, and coconut shell char in aqueous solutions. IOP Conference Series Earth Environmental Science. 208 (1), 012109, 2018.
- 44. MUTHURAJA R., OU B., THANGAVELU M., NARHAYANAN T.N., CHITTAMART N., JANJAROEN D. Effects of particle size and aging on heavy metal adsorption by polypropylene and polystyrene microplastics under varying environmental conditions. Chemosphere. 369, 143843, 2024.
- 45. MARIANA MULANA F., MUCHTAR S.H.K., FADHILAH A., FEBRINA C.Y. The utilization of activated carbon from Jamblang tree bark to adsorb lead heavy metal ion. IOP Conference Series Materials Science and Engineering. 1087 (1), 012062, 2021.
- 46. SIMÓN D., PALET C., CRISTÓBAL A. Cadmium removal by adsorption on biochars derived from wood industry and craft beer production wastes. Water. 16, 1905, 2024.
- 47. ALVES B.S.Q., FERNANDES L.A., SOUTHARD R.J. Biochar-cadmium retention and its effects after aging with hydrogen peroxide (H<sub>2</sub>O<sub>2</sub>). Heliyon. 7 (12), e08476, **2021**.
- 48. WANG L., GUO C., QIAN Q., LANG D., WU R., ABLIZ S., WANG W., WANG J. Adsorption behavior of UV aged microplastics on the heavy metals Pb(II) and Cu(II) in aqueous solutions. Chemosphere. 313, 137439, 2023.